文章编号：1006-9941(2020)01-0062-09

Simulation Dynamic Shock of Ignition Process on Solid Propellant with Quenched Combustion Method

ZHANG Huai-long[1], **WANG Yong**[2], **JIAN Xiao-xia**[1], **ZHOU Wei-liang**[1], **XIAO Le-qin**[1]

(1. *School of Chemical Engineering, Nanjing University of Science and Technology, Nanjing* 210094, *China*; 2. *Shanghai Space Propulsion Technology Research Institute, Shanghai* 201109, *China*)

Abstract: In order to study the effect of dynamic shock on solid propellant during the ignition process of solid rocket motor, a simulation setup based on quenched combustion was designed. The setup is composed of an ignition bolt, a combustion chamber, and a releasing pressure bolt. The metal burst disk is installed in the shear hole of the releasing pressure bolt and controls the ignition pressure precisely during the ignition shock process. Poly(BAMO-THF)/AP/Al solid propellant samples, molded into hollow cylinder, were used to evaluate the simulation shock process in setup. The *p-t* curves show that the blow-out pressure of burst disk is corresponding to the measured blow-out pressure in strong ignition mode and the pressure deviation is less than ±6%. The calculated pressurization rate according to the collected *p-t* curves can reach 7000 $MPa\cdot s^{-1}$ at 10 MPa ignition and 12000 $MPa\cdot s^{-1}$ at 15 MPa ignition, which are much more than the pressurization rate for actual ignition process of solid rocket. After simulation ignition shock experiment, filler particles implanted in the end face of propellant samples are damaged, while the inside surface basically keeps an intact condition. Compressive strength generally increases after ignition shock process, while the strain value at the point decreases when the compressive strength begins to rise. It is included that propellants with unstable structure are easier to be damaged and the mechanical properties would be changed during simulation ignition shock process.

Key words: solid propellant; simulation dynamic shock; quenched combustion; pressurization rate; compressive property

CLC number: TJ55; V435 **Document code:** A **DOI:** 10.11943/CJEM2019119

1 Introduction

Ignition of solid propellants is a complex process encompassing many physical and chemical features, such as unsteady heat conduction, surface chemistry and gas-phase combustion. Rapid pressurization of a solid rocket chamber during ignition transients will cause a prompt change of flow field and structural loadings that can probably result in much more cracks and defects [1-3]. The presence of cracks and defects, with large specific surface area, will accelerate the combustion of propellants. The process may produce intense compression waves or shock waves, which can induce detonation. As a result, it will have major implications for the combustion safety and reliability of propellant [4].

At present, many loading methods are used to model shock process in solid propellant, such as large drop hammer [5], Hopkinson Bar[6-7], and one-stage light gas gun loading device [8]. ZHENG[5] conducted the simulation shock experiment on azide polyether propellant by instrumented drop hammer at low temperature. It is found that when the loading shock energy is more than 2 J, the propellant samples will be broken. Through micro X-ray tomography technology of the propellant samples, crack propagation process is observed in the inner of the propellant samples which are broken up after the simulation shock experiments. Ho[6-7] studied the effect of shock

Received Date: 2019-05-06; **Revised Date:** 2019-07-20

Published Online: 2019-09-16

Project Supported: The National Basic Research Program of China (973 Program) (613275)

Biography: ZHANG Huai-long(1990-), male, doctoral candidate, majoring in the study of energetic materials. e-mail: zhhlchxjx@163.com

Corresponding author: JIAN Xiao-xia(1980-), female, doctor, majoring in the study of energetic materials. e-mail: jxx259@163.com

引用本文：张怀龙，王勇，菅晓霞，等. 中止燃烧方法模拟固体推进剂动态点火冲击过程[J]. 含能材料，2020，28(1):62-70.

ZHANG Huai-long, WANG Yong, JIAN Xiao-xia, et al. Simulation Dynamic Shock of Ignition Process on Solid Propellant with Quenched Combustion Method[J]. *Chinese Journal of Energetic Materials (Hanneng Cailiao)*, 2020, 28(1):62-70.

on solid propellant at different temperature through Hopkinson Bar experiments and developed a high strain-rate constitutive model for solid rocket propellant, including mechanical damage and nonlinear viscoelastic material response. Prediction made by the constitutive model has a good agreement with the results of experiments when the strain level is in the range from 30% to 40%. This model is able to predict the stress response quite reasonably outside the temperature range used to develop the constitutive equation, but inaccurately inside the range of the reduced strain-rate.

However, most experimental shock media mentioned above are solid and the loading speeds are lower, which are not close to the actual working conditions. Actually, ignition transient of solid propellant rocket is a very complicated process. At the ignition transient, the ignition materials will release huge clouds of gas and the pressure will increase sharply, which will strongly shock the propellant [9-13]. And the effect of the dynamic shock process will be coupled with temperature, especially ignited at the lower temperature [14]. In order to study the shock effect on solid propellant during the ignition process, the condition of simulation shock should be similar to the condition of actual ignition process.

In this paper, simulation dynamic shock of ignition process based on quenched combustion was used in low-temperature poly(BAMO-THF)/AP/Al propellant to simulate the actual ignition process. For good repeatability, the simulation ignition shock experiment is performed at different ignition conditions, including the ignition mode, ignition pressure and sample temperature, to investigate the developing of pressure and pressurization rate during ignition shock process. Furthermore, the morphology and the compression property of propellants were studied by 3D video microscope and universal material testing machine, respectively.

2 Experimental

2.1 Simulation Ignition Shock Principles

The simulation ignition shock experiment with controllable pressure is used in propellant quenched combustion experiment principle[15]. The ignition material was first ignited by electric ignition and produced a lot of high-temperature and high-pressure gas instantaneously. As a result, the propellant sample is shocked by the high pressure gas. When the pressure in the combustion vessel exceeded the limit pressure, at which burst disk can just hold up, the burst disk would blow out and the combustion would quench, due to the instantaneous decrease of pressure. At last, the propellant was collected for further investigation. The shock process is given in Fig. 1.

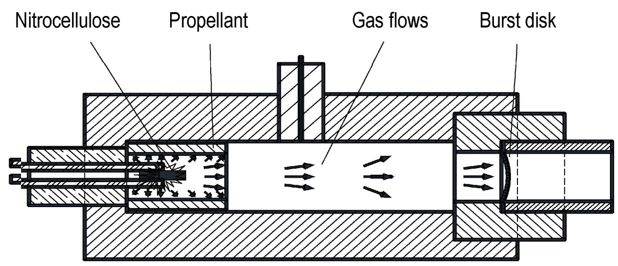

Fig. 1 Schematic depiction of the simulation ignition shock experiment

2.2 Experimental Setup

The experiment of simulation ignition shock of solid propellant is carried out under semi-closed bomb, as seen in Fig. 2. The semi-closed bomb setup consists of an ignition bolt, a combustion chamber, and a releasing pressure bolt with a metal burst disk in the shear hole. The electric igniter consisting of a certain amount nitrocellulose powder and a fuse connected to the electrodes is assembled in the ignition bolt. A pressure gauge is installed into the side of the combustion chamber. The metal burst disk is intended to terminate the combustion when the pressure rises to the required value.

For the simulation ignition shock setup, blow-out pressure is controlled by metal burst disk, which

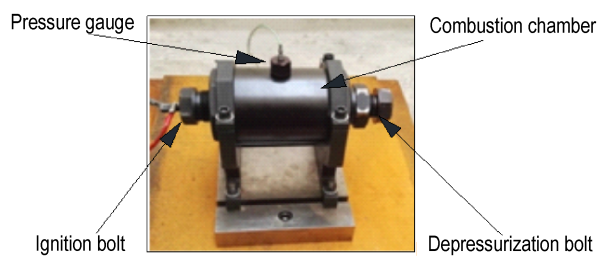

Fig. 2 Photograph of simulation ignition shock apparatus

is installed into the depressurization pressure bolt. The metal burst disk is made by stainless steel and is arch shaped with indenting on the surface. The blow-out pressure of the burst disk is controlled by the arch diameter and highness when the material remains unchanged. In order to get close to the real working pressure of the solid rocket motor, three types of burst disks with different blow-out pressure (5 MPa, 10 MPa and 15 MPa) were designed and machined, as shown in Fig. 3.

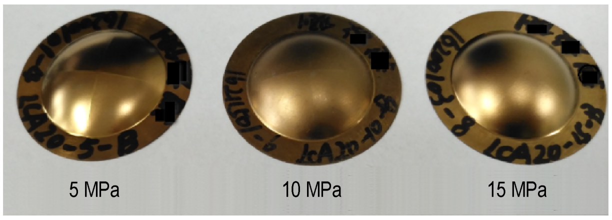

Fig. 3 The scheme of burst disk of different pressures

2.3 Propellant Samples

The solid propellant used in this study mainly contains 3,3-bis (azidomethyl) oxetane and tetrahydrofuran copolyether (poly(BAMO-THF)), ammonium perchlorate (AP), aluminum powder (Al) and is manufactured by the casting method, comprising of 75% solid particles (AP/Al), 10% poly(BAMO-THF) binder, and 15% others. The density of the poly (BAMO-THF)/AP/Al propellant is about 1800 $kg \cdot m^{-3}$.

To ensure the propellant samples stay in the combustion chamber after ignition shock process, the hollow cylinder is an appropriate choice for propellant samples. The hollow structure can make the combustion gas go through and the direction of the gas shock is mainly the radial during the ignition shock process, as shown in Fig. 1. To manufacture the propellant samples with hollow structure, ten moulds (Fig. 4) was designed and the casting method were used by these moulds. The outer diameter of the propellant samples agrees with the inside diameter of the combustion chamber. Before the simulation ignition shock experiments, the propellant samples would be cut into smaller samples. The dimensions and shapes of the propellant samples are shown in Fig. 5. The propellant samples would be used in all simulation ignition shock experiments. Before the experiments, the propellant samples would be kept at -40 °C or -20 °C for about 48 h.

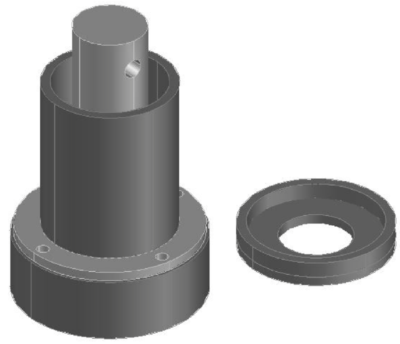

Fig. 4 Mould for manufacturing the propellant samples

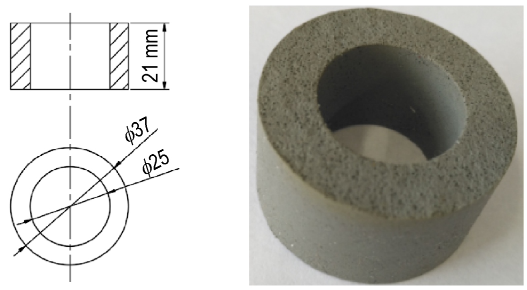

Fig. 5 Geometrical shape and the sample of poly(BAMO-THF)/AP/Al propellant

2.4 Mass of Ignition Material

In the simulation ignition shock experiment, the increase of pressure is dependent on the combustion of ignition material. The mass of ignition material needs to satisfy the blow-out pressure. Because the ignition shock setup is close to the closed bomb before the burst disk blowing out, the calculation of the ignition material mass refers to the formula used in the closed bomb experiment [16].

$$m_i = \frac{p_t(V - m/\delta)}{f_i + p_t\alpha_i} \qquad (1)$$

where m_i is the mass of ignition material, kg, nitrocellulose is used in this study; V is the volume of combustion chamber, m^3, the volume in this study is 100 cm^3; p_t is the theoretical ignition pressure, Pa; δ is the density of propellant, $kg \cdot m^{-3}$, azide propellant in this study is 1800 $kg \cdot m^{-3}$; f_i is the ignition material power, $J \cdot kg^{-1}$; α_i is the real volume of ignition material per unit mass, $m^3 \cdot kg^{-1}$.

Using this formula, the mass of ignition materials can be calculated at a certain pressure. Herein, two ignition methods with different mass of ignition material were adopted. One is called the weak ignition mode, in which the theoretical pressure is in accordance with the blow-out pressure (p_b) of the burst disk. The other is the strong ignition mode, in which the theoretical pressure is beyond to the blow-out pressure of the burst disk. The calculated results are shown in Table 1.

Table 1 The relationship of ignition pressure and ignition materials

ignition mode	p_t / MPa	p_b / MPa	m_i / g
weak ignition	5	5	0.50
	10	10	0.98
	15	15	1.79
strong ignition	7	5	0.85
	13	10	1.56
	17	15	2.03

2.5 Characteristic of Propellant Samples

(1) The micrograph of propellant samples

A 3D video microscope (Questar HiROX KH-100, America) was used to observe the micrograph of the propellant samples before and after the ignition shock experiments under the magnification of 50 times and 200 times.

(2) Characteristic of the compressive property of propellant samples

A universal material testing machine (Instron3367, America) was used to study the compressive property of propellant samples. The measurement was conducted at −40 ℃ at the condition of 10 mm·min^{-1} compressive rate. The compressive stress-strain curves were obtained from the tests. Before the test, the propellant samples would be kept in −40 ℃ for 48 h in the low temperature oven.

3 Results and Discussion

3.1 Choice of the Ignition Mode

3.1.1 Weak Ignition

Simulation ignition shock experiment was firstly conducted in the weak ignition mode at 10 MPa to test the feasibility of this method. Fig.6 shows the p-t curves and dp/dt-t curves of ignition shock process at 10 MPa ignition pressure. The diagram of w-T(−40)-p(10)-1 is named in the order: ignition mode, sample temperature, blow-out pressure and experiment number. That is to say, w-T(−40)-p(10)-1 means the first experiment of weak ignition mode under the condition of −40 ℃ propellant temperature and 10 MPa blow-out pressure. The following experimental diagrams are named in this rule.

The p-t curves and dp/dt-t curves of simulation ignition shock process are seen in Fig.6. The pressures of two tests at 10 MPa are 8.994 MPa and 8.803 MPa, respectively, which are lower than the blow-out pressure, as shown in Table 2. The pres-

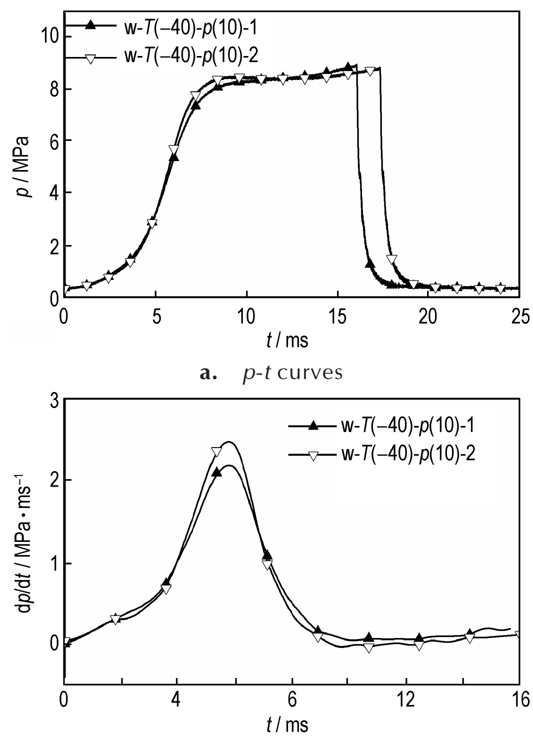

a. p-t curves

b. dp/dt-t curves

Fig. 6 p-t curves and dp/dt-t curves of weak ignition at 10 MPa and −40 ℃

Table 2 Experimental data of weak ignition shock experiments

samples	T_m / ℃	p_b / MPa	p_m / MPa	D / %	t_m / ms
w-T(−40)-p(10)−1	−40	10	8.994	−10.06	26.72
w-T(−40)-p(10)−2	−40	10	8.803	−11.97	25.43

Note: T_m is temperature of propellant sample; p_b is blow-out pressure of burst disk. p_m is measured blow-out pressure; D is pressure deviation; t_m is time from the beginning to the peak of the pressure.

sure deviation is more than 10%, and the ignition time is over 25 ms. The pressurization rate is up to 2000 $kPa\cdot s^{-1}$, according to the d*p*/d*t*-*t* curves. We can see that two effects might decrease the blow-out pressure. Firstly, due to the very low temperature of propellant sample, massive energy lost, resulting in the decrease of the pressure. The other one is that the ultimate strength of the burst disk would decline with long time impacting by the high-temperature and high-pressure gas. From the *p*-*t* curves in Fig.6, it is found that the curves will continue to rise before the burst disk blowing out, suggesting that the propellants are ignited. It should avoid the ignition of the propellant during the ignition shock process, which will disturb the study of the influence of the shock process on propellants.

3.1.2 Strong Ignition

The tested *p*-*t* curves are shown in Fig.7a and the calculated d*p*/d*t*-*t* curves are shown in Fig.7b. The experimental data of strong ignition are shown in Table 3. In Fig.7a, the pressures of the two tests increase dramatically, and the burst disks of two experiments both crack is about 3 ms after the ignition. According to Fig.7b, the calculated pressurization rate can get to 7000 $MPa\cdot s^{-1}$, which is over 3 times than that of weak ignition. As shown in Table 3, the pressure deviation is much lower, only about ±1.2%. Hence, the blow-out pressure in strong ignition mode can be regarded as the ignition pressure.

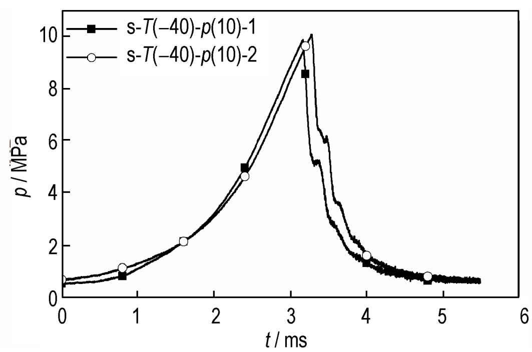

a. *p*-*t* curves

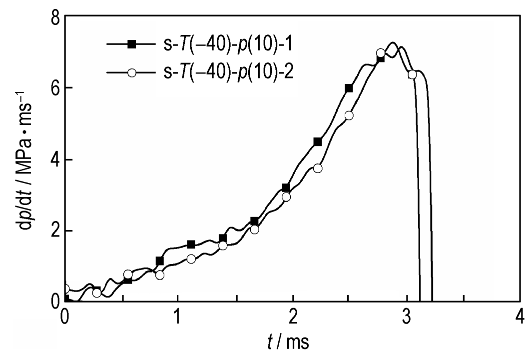

b. d*p*/d*t*-*t* curves

Fig. 7 *p*-*t* curves and d*p*/d*t*-*t* curves of the strong ignition at ignition pressure of 10 MPa and sample temperature of−40 ℃

Table 3 Experimental data of the strong ignition

samples	T_m / ℃	p_b / Pa	p_m / MPa	*D* / %	t_m / ms
s-*T*(−40)-*p*(10)−1	−40	10	9.89	−1.1	3.16
s-*T*(−40)-*p*(10)−2	−40	10	10.12	1.2	3.28

Comparing the two ignition modes, it is found that the measured blow-out pressure is in accordance with the blow-out pressure of bust disk, and there is no other effect factor on propellant samples exists in the strong ignition. It is concluded that the strong ignition is suitable for the ignition shock experiment.

3.2 Repeatability Testing of Simulation Ignition Shock

From the curves in Fig.7, we can find that the curves of strong ignition at 10 MPa ignition pressure have good repeatability. In order to verify the repeatability of simulation ignition shock method at higher pressure, we performed five ignition experiments to poly(BAMO-THF)/AP/Al propellant samples (−40 ℃ for 48 h) at 15 MPa blow-out pressure. The collected *p*-*t* curves are shown in Fig.8.

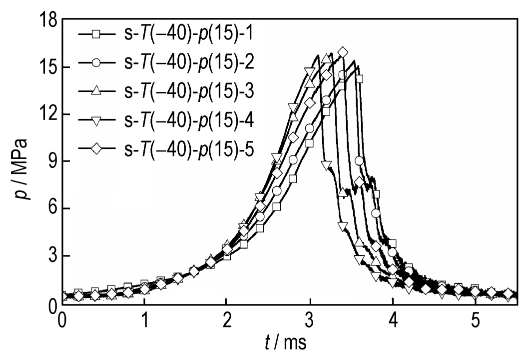

Fig. 8 *p*-*t* curves of five ignition experiments (−40 ℃) at blow-out pressure of 15 MPa

In Fig.8, the pressure increases rapidly in *p*-*t* curves because of the burning of the nitrocellulose, this increase is followed by an increase of the vessel pressure in time, and the measured pressure values are at the range of 15.0−15.9 MPa. Then the pressure drops rapidly due to the crack of the burst disks. Pressure deviation is less than ±6% compared to the blow-out pressure 15 MPa, as shown in Table 4. And the ignition times from the beginning to the peaks of the pressure are basically equal, the corresponding blow-out times are close, which means that the measured pressure is within the deviation range of the blow-out pressure and the pressure is controllable and repeatable.

Table 4 Details of simulation ignition shock of different poly (BAMO-THF)/AP/Al propellant samples

samples	T_m / ℃	p_b / MPa	p_m / MPa	D / %	t_m / ms
s-T(−40)-p(15)-1	−40	15	15.0	0	3.6
s-T(−40)-p(15)-2	−40	15	15.4	2.67	3.5
s-T(−40)-p(15)-3	−40	15	15.8	5.33	3.3
s-T(−40)-p(15)-4	−40	15	15.7	4.67	3.1
s-T(−40)-p(15)-5	−40	15	15.9	6.00	3.4

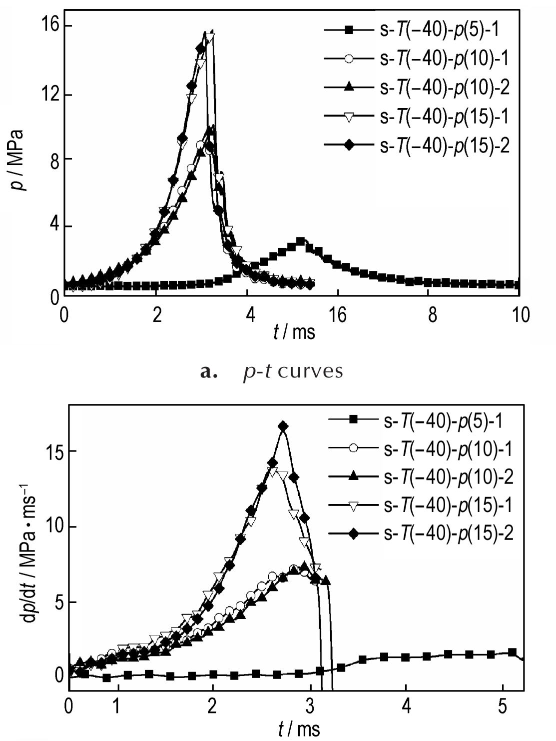

a. p-t curves

b. dp/dt-t curves

Fig. 9 p-t curves and dp/dt-t curves at different ignition pressures

3.3 p-t and dp/dt-t Curves at Different Ignition Pressure

Simulation ignition shock experiment was conducted to evaluate the effect of ignition pressure on propellant sample. The collected p-t curves and calculated pressurization rate (dp/dt-t curves) are shown in Fig. 9. As seen in Fig. 9a, the values of the blow-out pressure of s-T(−40)-p(15)-1, s-T(−40)-p(15)-2, s-T(−40)-p(10)-1 and s-T(−40)-p(10)-2 are 15.0, 15.4, 9.93 MPa and 10.12 MPa, respectively. It is found that the measured blow-out pressures at 15 MPa and 10 MPa are basically consistent with the blow-out pressure. However, the measured blow-out pressure of s-T(−40)-p(5)-1 sample is just 3.15 MPa. Moreover, four curves at 15 MPa and 10 MPa almost get to the peak at the same time, while the curve of s-T(−40)-p(5)-1 sample has longer ignition delay time. It is analyzed that the less nitrocellulose may be not enough to generate plenty of gas, and the longer ignition delay time may decrease the ultimate strength of the burst disk.

According to Fig. 9b, the different blow-out pressure has a great influence on the rate of gas pressurization. Pressurization rate can get to 1500 MPa·s^{-1} at 5 MPa ignition, 7000 MPa·s^{-1} at 10 MPa ignition and 12000 MPa·s^{-1} at 15 MPa ignition respectively, and all of them are higher than the real motor ignition rate. From Fig. 9b, the pressurization rate of s-T(−40)-p(5)-1 sample is almost unchanged during the pressure increasing process, while the pressurization rates at 10 MPa ignition and 15 MPa ignition increase apparently. It is explained that the mass of the gas produced from the combustion of nitrocellulose at 5 MPa is much less and the combustion time of nitrocellulose has little difference with the combustion time at 10 MPa and 15 MPa.

3.4 p-t and dp/dt-t Curves at Different Propellant Temperatures

The influence of the propellant temperature on the ignition shock process is also investigated. Before the experiment, the propellant samples were conditioned at −20 ℃ and −40 ℃ for 48 h, respectively, and carried out the simulation ignition experiment at 10 MPa. As can be seen from Fig. 10a, the pressure peak values in p-t curves all basically get to 10 MPa. The difference is that the delay time of −20 ℃ pro-

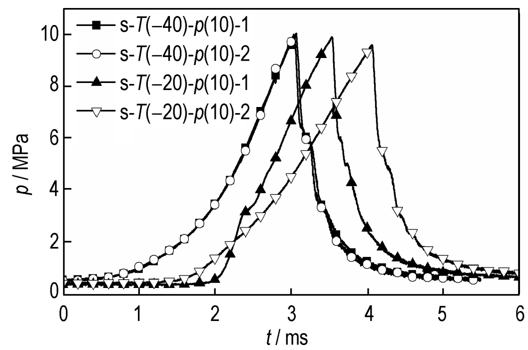

a. *p*-*t* curves

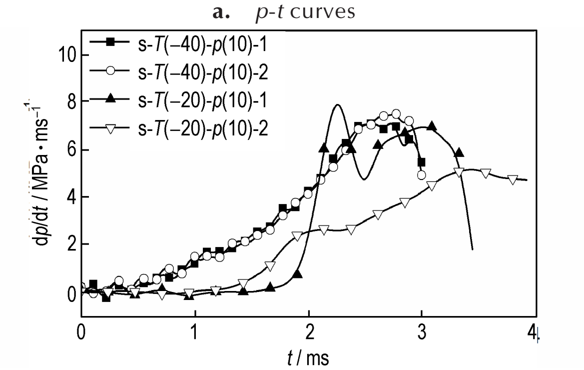

b. d*p*/d*t*-*t* curves

Fig. 10 *p*-*t* curves and d*p*/d*t*-*t* curves of poly(BAMO-THF)/AP/Al propellant at different temperatures

pellant sample is longer than that of −40 ℃ propellant sample. Comparing the d*p*/d*t*-*t* curves from Fig. 10b, it is shown that the pressurization rate of −40 ℃ propellant sample is higher than that of the −20 ℃ propellant sample. That is to say, it is easier to be ignited for nitrocellulose at −40 ℃. While it is known that nitrocellulose is easier to be ignited as the environment temperature is higher [17]. Apparently, the result is opposite according to Fig. 10b. The reason may be ascribed to the human factors during the experiment process or other unknown factors, which needs further experiments to verify.

3.5 Effects on Propellant Micro Morphology by Ignition Shock Process

The pristine sample and s-*T*(−40)-*p*(10)-1 sample were observed according to the method in section 2.6. For comparison, the end face and the inside surface of propellant samples were taken as the observation point. The end face of the propellant sample is a damaged surface, which was injured during the preparation process of the samples, while the inside surface of the sample keeps an intact structure, without any damage. Fig.11 and Fig.12 show the end face and inside surface micrographs of pristine sample and s-*T*(−40)-*p*(10)-1 sample, respectively.

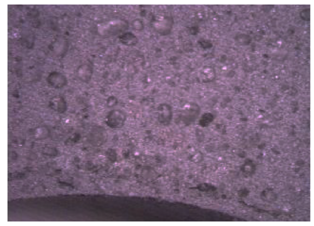

a. pristine sample (50×)

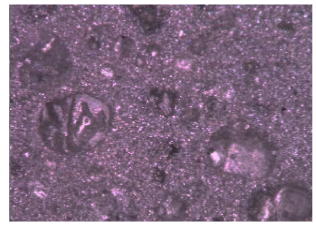

b. pristine sample (200×)

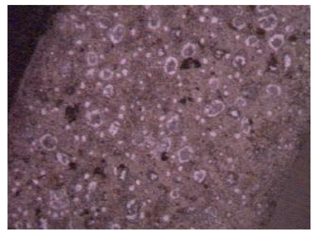

c. s-*T*(−40)-*p*(10)-1 sample(50×)

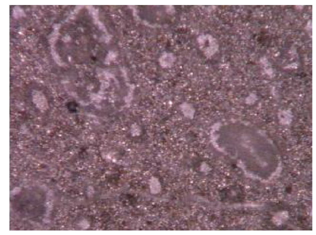

d. s-*T*(−40)-*p*(10)-1 sample (200×)

Fig. 11 The end face micrograph of propellants before and after ignition shock

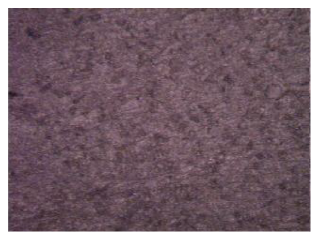

a. pristine sample (50×)

b. pristine sample (200×)

c. s-*T*(−40)-*p*(10)-1 sample (50×)

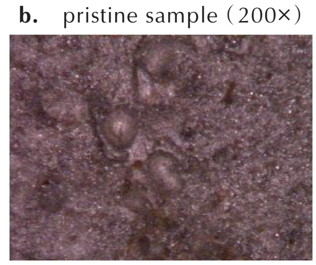

d. s-*T*(−40)-*p*(10)-1 sample (200×)

Fig. 12 The inside surface micrograph of propellant samples before and after ignition shock.

Most filler particles on the end face of pristine sample (Fig.11a and Fig.11b) keep an intact state, except that a few were damaged by knife cutting in the process of sample preparation. However, most filler particles on the end face (Fig.11c and Fig.11d) are surrounded by white circles, and some have white points in the middle of the particles, which indicates that the filler particles burned or broken during the ignition shock process. As the particles on the end face were cut by a knife in sample preparation or shocked by external mechanical force, lots of micro cracks will be generated. During the ignition shock process, particles will be broken as the shock accelerates the crack growth.

According to Fig.12, the inside surface of pristine sample (Fig.12a and Fig.12b) is flat and the particles are implanted in the surface. After ignition shock process, the inside surface (Fig. 12c and Fig.12d)) still keeps an intact structure. Comparing Fig.12b with Fig.12d, it is found that a few particles are exposed outside after the ignition shock experiment, which indicates that the polymer matrix of inside surface was burned during the ignition process.

Two different phenomena could ascribe to the different structures of the two surfaces. The structure of the inside surface is very stable and has no damage before ignition-shock experiment, while the structure of the end face has a rough surface and a lot of unstable structures caused by the damage before the experiment. When high-temperature high-pressure gas flow scoured from the surface, unstable structure would be damaged and the particles would be fractured during the process. It means that the damaged structure is easier to be damaged during the ignition shock process.

3.6 Effect of Ignition Pressure and Propellant Temperature on Compressive Strength

Fig.13 shows the tested compressive stress-strain curves of the samples. It clearly demonstrates that the compressive strength is generally improved after ignition shock. The compressive strength keeps a stage at the beginning. For the pristine sample, when the strain is up to 10%, the compressive strength start to rise. The value of s-T(−40)-p(10)−1 sample is about 6% and the value of s-T(−40)-p(15)−1 sample is about 4%. This indicates that the elasticity of the propellant decreases with the ignition pressure increasing. When the strain continues to increase, the compressive strength of propellants will increase with the increasing of ignition pressure. Because the ignition shock occurs in mainly radial direction, some microstructure may orientate in a direction, resulting in the strain rate enhancement effect by ignition shock[18].

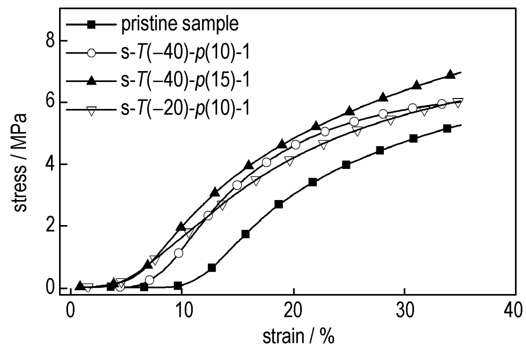

Fig. 13 Compressive stress-strain relationship of the sample

Comparing the curves of s-T(−40)-p(10)-1 and s-T(−20)-p(10)-1, the tendency of the two curves almost coincides when the strain value is less than 35%. There is little difference in compressive strength when the temperature of propellant is different in the ignition shock process. It is indicated that the temperature of propellant samples in the ignition shock process has little influence on the compressive strength.

4 Conclusions

(1) The experimental apparatus established is able to simulate the dynamic shock of ignition process on solid propellant. The blow-out pressure of burst disk is within the deviation range according to the p-t curves, and the pressure is controllable and repeatable. The pressurization rate was calculated, which can get to 7000 MPa·s^{-1} at 10 MPa ignition and 12000 MPa·s^{-1} at 15 MPa ignition respectively, and higher than the pressurization rate of actual ignition process of rocket motor.

(2) The filler particles on the end face of propellant samples are burned or broken during the ignition shock process. While the inside surface still keeps an intact state after ignition shock experiment. Propellants with unstable structure are easier to be damaged during the ignition shock process.

(3) The compressive strength of propellant sample after being shocked is generally improved. For the pristine sample, s-T(−40)-p(10)−1 sample and s

-T(−40)-p(15)−1 sample, the strain value at the point of the compressive strength starting to rise is 10%, 6% and 4%, respectively. It means that the elasticity of the propellants decreases with the increase of ignition pressure.

References:

[1] Arkhipov V A, Zolotorev N N, Korotkikh A G. Dynamic ignition regime of condensed system by radiate heat flux [J] *Journal of Physics: Conference Series*, 2017, 830(1): 1−9.

[2] Glushkov D O, Kuznetsov G V, Strizhak P A. Ignition of a polymer propellant of hybrid rocket motor by a hot particle [J]. *Acta Astronautica*, 2017, 133: 387−396.

[3] Shaw R W, Brill T B, Thompson D L. Advanced Series in Physical Chemistry Volume 16: Overviews of Recent on Energetic Materials [M]. Singapore: World Scientific Publishing Co.Pte. Ltd, 2005: 369−417.

[4] Parker G R, Peterson P D, Asay B W, et al. Examination of morphological changes that affect gas permeation through thermally damaged explosives [J]. *Propellants, Explosives, Pyrotechnics*, 2004, 29(5): 274 - 281.

[5] ZHENG Qi-long, LIU Hai-tao, HU Yi-wen, et al. Impact damage and dynamic mechanical behaviors of azido polyether propellant at low temperature [J]. *Chinese Journal of Energetic Materials* (*Hanneng Cailiao*), 2017, 25(5): 354−359. In Chinese

[6] Ho S Y. High Strain-rate constitutive models for solid rocket propellant [J]. *Journal of Propulsion and Power*, 2002, 18 (5): 1106−1111.

[7] Ho S Y, Fong C W. Correlation between fracture properties and dynamic mechanical relaxations in composite propellants [J]. *Polymer*, 1987, 28(5), 739−744.

[8] HUANG Feng-lei, WANG Ze-ping, DING Jing. Dynamic fracture of composite solid propellant [J]. *Acta Armamentarii* (*Binggong Xuebao*), 1995, 17(2): 47−50.

[9] Glushkov D O, Kuznetsov G V, Strizhak P A. Calculation of the characteristics of the ignition of a metallized composite propellant using various methods for describing its thermophysical properties [J]. *Russian Journal of Physical Chemistry B*, 2017, 11(1):133−139.

[10] Glushkov D O, Kuznetsov G V, Strizhak P A. Effect of the thermophysical properties of the material of a local energy source on conditions and characteristics of ignition of metallized composite propellants [J]. *Russian Journal of Physical Chemistry B*, 2016, 10(6): 946−952.

[11] Glushkov D O, Kuznetsov G V, Strizhak P A. Ignition of a metallized composite solid propellant by a group of hot particles [J]. *Combustion, Explosion, and Shock Waves*, 2016, 52 (6): 694−702.

[12] Shiang-Woei Chyuan. Dynamic analysis of solid propellant grains subjected to ignition pressurization loading [J]. *Journal of Sound and Vibration*, 2003,268(3): 465−483.

[13] Beckstead M W, Puduppakkam K, Thakre P, et al. Modeling of combustion and ignition of solid-propellant ingredients [J]. *Progress in Energy and Combustion Science*, 2007, 33(6): 497−551.

[14] Balzer J E, Siviour C R, Walley S M, et al. Behavior of ammonium perchlorate-based propellants and a polymer-bonded explosive under impact loading [J]. *Proceedings of the Royal Society A*, 2004, 460(2043): 781−806.

[15] YE Zhen-wei, YU Yong-gang. Numerical simulation of quenched combustion model for AP/HTPB propellant under transient depressurization [J]. *Propellants, Explosives, Pyrotechnics*, 2017, 42(9): 1085−1094.

[16] XIAO, Zheng-gang, YING San-jiu, XU Fu-ming. Response of TEGDN propellants to plasma ignition with the same magnitude of ignition energy as conventional igniters in an interrupted burning simulator [J]. *Propellants, Explosives, Pyrotechnics*, 2015, 40(4): 484−490.

[17] LI Lu, ZHOU Fu-guo, LI Yi-min. Research on ignition characteristics of high-energy igniters [J]. *Journal of Aerospace Power*, 1991, 6(2): 105−110.

[18] Peterson P D, Mang J T, Fletcher M A, et al. Influence of Pressing Parameters on the Microstructure of PBX 9501 [J]. *American Institute of Physics Conference Proceedings*, 2004, 706(1): 796−799.

中止燃烧方法模拟固体推进剂动态点火冲击过程

张怀龙[1],王　勇[2],菅晓霞[1],周伟良[1],肖乐勤[1]

(1. 南京理工大学化工学院,江苏 南京 210094; 2. 上海航天动力技术研究所,上海 201109)

摘　要: 为了研究火箭发动机点火过程中动态冲击对固体推进剂的影响,设计了一个基于中止燃烧的模拟点火冲击装置。该装置由点火螺栓、燃烧室和泄压螺栓组成。金属爆破片安装在泄压螺栓的剪切口处,在点火冲击过程中准确控制泄压压力。模拟点火冲击试验的研究对象是圆环柱体形状的poly(BAMO-THF)/AP/Al固体推进剂试样。*p-t*曲线表明爆破片的泄压压力与测得的压力一致,其误差在±6%。根据*p-t*曲线计算增压速率,10 MPa下增压速率达到7000 $MPa\cdot s^{-1}$,15 MPa下增压速率达到12000 $MPa\cdot s^{-1}$,这远远大于固体火箭实际点火过程中的增压速率。在模拟点火冲击试验后,推进剂试样端面(受损表面)镶嵌的粒子受损,而内侧表面(未损表面)仍保持完整的状态。点火冲击试验后,推进剂试样的压缩强度增加,而压缩强度开始增加时的形变值降低。这说明在模拟点火冲击试验后,推进剂受损表面会进一步受损,力学性能也会发生改变。

关键词: 固体推进剂;模拟点火冲击;中止燃烧;增压速率;压缩性能

中图分类号: TJ55;V435　　**文献标志码:** A　　**DOI:**10.11943/CJEM2019119

(责编:王艳秀)